行政院國家科學委員會專題研究計畫　期中進度報告

銅-(錳、鎳)-鋁合金相變化(1/2)

計畫類別：個別型計畫
計畫編號：NSC92-2216-E-009-026-
執行期間：92 年 08 月 01 日至 93 年 07 月 31 日
執行單位：國立交通大學材料科學與工程學系

計畫主持人：劉增豐

報告類型：精簡報告

處理方式：本計畫可公開查詢

中　華　民　國 93 年 5 月 26 日

行政院國家科學委員會補助專題研究計畫 ☐ 成 果 報 告 ☑ 期中進度報告

Phase Transformations in a Cu-28Mn-24Al Alloy

計畫類別：☑ 個別型計畫　　☐ 整合型計畫
計畫編號：NSC92－2216－E－009－026
執行期間：　92 年　8 月　1 日至　93 年　7 月 31 日

計畫主持人：劉增豐 教授
共同主持人：
計畫參與人員：

成果報告類型(依經費核定清單規定繳交)：☑ 精簡報告　☐完整報告

本成果報告包括以下應繳交之附件：
☐赴國外出差或研習心得報告一份
☐赴大陸地區出差或研習心得報告一份
☐出席國際學術會議心得報告及發表之論文各一份
☐國際合作研究計畫國外研究報告書一份

處理方式：除產學合作研究計畫、提升產業技術及人才培育研究計畫、列管計畫及下列情形者外，得立即公開查詢
☐涉及專利或其他智慧財產權，☐一年☐二年後可公開查詢

執行單位：國立交通大學料科學與工程學系

中　華　民　國　93　年　5　月　26　日

行政院國家科學委員會補助專題研究計劃成果報告

Phase Transformations in a Cu-28Mn-24Al Alloy

計劃編號：NSC92-2216-E-009-026

執行期限：92 年 08 月 01 日至 93 年 07 月 31 日

主持人：劉增豐　國立交通大學材料科學及工程學系

一、中文摘要

在淬火狀態下，Cu-28Mn-24Al 合金的微結構為(L2₁+B2+L-J)的混和相，這個結果和以往在 $Cu_{3-x}Mn_xAl$ (0≦x≦1)合金中所觀察到的有所不同。當此合金在 400°C 做時效處理後，會有層狀的 γ - brass 及 β - Mn 在 L2₁ 基地中析出，這個結果未曾在 Cu-Al，Cu-Mn 和 Cu-Mn-Al 合金中被發現過。

在此合金經過 300 到 750°C 長時間的時效處理後，其相變化過程為(B2+L2₁+L-J)→(L2₁+γ-brass+β-Mn)→(γ-brass+β-Mn)→(L2₁+β-Mn)→(B2+L2₁+L-J)，此結果從未在 Cu-Mn-Al 合金中被發現。

關鍵字：銅鋁錳合金、相變化

● Abstract

In the as-quenched condition, the microstructure of the Cu-28Mn-24Al alloy was a mixture of ($L2_1$+B2+L-J) phases. This result is quite different from that observed in the $Cu_{3-x}Mn_xAl$ ($0 \leqq x \leqq 1$) alloys. When the alloy was aged at 400°C, γ- brass and β- Mn with a lamellar structure were observed within the $L2_1$ matrix. The coexistence of the (γ-brass +β-Mn) phases has never been observed by other workers in the Cu-Al, Cu-Mn and Cu-Mn-Al alloy systems before.

When the as-quenched alloy was aged at temperature ranging from 300 to 750°C for long times, the phase transition sequence as the aging temperature was found to be (B2+$L2_1$+L-J) → ($L2_1$+γ-brass+β-Mn) → (γ-brass+β-Mn) → ($L2_1$+β-Mn) → (B2+$L2_1$+L-J).This transformation has also never been observed by other worker in the Cu-Mn-Al alloy systems before.

Keywords: Cu-Al-Mn alloy, phase transformation

二、Introduction

Phase transformations in $Cu_{3-x}Mn_xAl$ alloys have been studied by many workers [1-6]. Based on these studies, M. Bouchard and G. Thomas has established that the $Cu_{3-x}Mn_xAl$ alloys with $0.2 \leqq x \leqq 0.8$ were solution heat-treated in the single β phase field and then quenched into iced brined rapidly, a β→B2→$D0_3$+$L2_1$ phase transition occurred during quenching [1] .When the manganese content in the $Cu_{3-x}Mn_xAl$ alloy was increased to 25 at. pct (x=1), the as-quenched microstructure became a single $L2_1$ phase [1-3]. Based on our study, the microstructure of the $Cu_{2.2}Mn_{0.8}Al$ alloy in the as-quenched condition or aged at 300°C was a mixture of ($D0_3$+$L2_1$+L-J) phases[7]. The L-J phase had an orthorhombic structure with lattice parameter a=0.413nm, b=0.254nm and c=0.728nm. The L-J phase was never be found in the Cu-Al, Cu-Mn and Cu-Mn-Al alloy systems by other workers before.

When the $Cu_{3-x}Mn_xAl$ alloys were aged at temperatures at 450°C or below, the γ-brass precipitated within the $L2_1$ (or $D0_3$+$L2_1$) matrix [3-6]. The γ-brass precipitate has a $D8_3$(ordered body-centered cubic) structure with lattice parameter a=0.872nm [3-4]. The orientation relationship between the γ-brass and the matrix was cubic to cubic [6]. As the aging temperature was increased in the range from 460°C to 650°C, the γ-brass disappeared and β-Mn precipitated in the matrix, that the β-Mn precipitate has a A13 (simple cubic) structure with lattice parameter a=0.641nm [3-4]. Recently, we have also used TEM observation on the phase transformations of the Cu_2MnAl alloy. In this study , it is found that when the alloy was aged at 460°C and 560°C, the β-Mn were found to be formed in the $L2_1$ matrix with plate-like shape and granular shape, respectively. Through electron diffraction analyses identified that in spite of the morphology change the orientation relationship between the β-Mn and $L2_1$ matrix would still maintain the same, and it could be described as follows: $(210)_{\beta\text{-}Mn}$ //$(100)_m$, $(120)_{\beta\text{-}Mn}$ //$(100)_m$ and $(001)_{\beta\text{-}Mn}$ //$(001)_m$. [8]. The result is inconsistent with that proposed by R. Kozubski et al.[6] in the aged Cu_2MnAl alloy.

Up to date, the research of the phase transformations in a Cu-Mn-Al alloys have been focused on the $Cu_{3-x}Mn_xAl$ alloys with $0 \leqq x \leqq 1$. Information concerning the microstructure of the Cu-Mn-Al alloy with higher manganese content(exceed 25 at. pct) is very deficient. Therefore, the purpose of this present work is to investigate the microstructure of the Cu-28 at. pct Mn-24 at. pct Al alloy.

三、Experimental Procedure

The alloy, Cu-28 at. pct Mn-24 at. pct Al, was prepared in an induction furnace by using 99.9 pct copper, 99.9 pct manganese and 99.9 pct aluminum. The ingot was re-melted at 1000℃in an argon atmosphere and then chill cast into a 30x50x200 ㎜ copper mold. After being homogenized at 900℃ for 72 hours, the ingot was sectioned into 2.0 ㎜ slices in thickness. These slices were subsequently solution heat-treated at 900℃ for 1 hour and then quenched into iced brine. The aging processes were performed at the temperature ranging from 300℃ to 750℃for various times in a vacuum heat-treated furnace.

Electron microscopy specimens were prepared by means of a double-jet electropolisher with an electrolyte of 70 percent methanol and 30 percent nitric acid. The polishing temperature was kept in the range from -30℃ to -15℃, and the current density was kept in the range from $3.0x10^4$ to $4.0x10^4$ A/m^2. Electron microscopy was performed on a JEOL* JEM-2000FX scanning transmission electron microscope operating at 200 KV. This microscope was equipped with a Link ISIS 300 energy-dispersive X-ray spectrometer (EDS) for chemical analysis. Quantitative analyses of elemental concentrations for Cu, Mn and Al were made with the aid of a Cliff-Lorimer Ratio Thin Section method.

*JEOL is a trademark of Japan Electron Optics Ltd., Tokyo.

四、Results

Fig. 1(a) is a bright field (BF) electron micrograph of the as-quenched alloy, revealing the presence of fine precipitates within the matrix. Fig. 1(b)-(c) are two different selected-area diffraction patterns (SADPs) of the as-quenched alloy. When compared to our previous study in the $Cu_{2.2}Mn_{0.8}Al$ alloy [7], it is found in these SADPs that in addition to the brighter and well-arranged reflection spots are of the ordered $L2_1$ phase, and the extra spots with streaks are derived from the L-J phase. Although these reflection spots could be analyzed as a single $L2_1$ phase, the $L2_1$ reciprocal lattices contain all the B2-type reflections[9-11]. In our previous study[12], it was found that the intensity of the (111) and (200) reflection spots of a single $L2_1$ phase should be almost equivalent. However, it is clearly seen in Figure 1(c) that the (002) and $(\bar{2}22)$ reflection spots are much stronger than the (111) reflection spots. Therefore, it is strongly suggested that the (002) and (222) reflection spots in Figures 1(b) and (c) should derived from not only $L2_1$ phase but also the B2 phase. Fig. 1(d) is a $(\bar{1}11)$ $L2_1$ DF electron micrograph of the same area as Fig. 1(a), shows that in addition to the L-J precipitates (as indicated by arrows), a high density of extremely dark flecks (marked as "F") could be observed within the $L2_1$ domain. Fig 1(e), a (002) $L2_1$ DF electron micrograph that shows the dark flecks become bright in contrast. Fig. 1 (f) is a $(0\ \bar{2}\ 0_1)$ L-J dark field (DF) electron micrograph, revealing the presence of fine L-J precipitates. Based on the above observations, it is concluded that the microstructure of the alloy in the as–quenched condition was a mixture of ($L2_1$+B2+ L-J) phases.

When the as-quenched alloy was aged at 300℃ or below and then quenched, the size of the B2 precipitates were increased with the aged times, as illustrated in Fig. 2. However when the aging temperature was increased to 400°C, two kinds of precipitates with a lamellar structure started to appear within the $L2_1$ matrix. A typical example is shown in Fig. 3(a), which is a BF electron micrograph of a specimen aged at 400°C for 2 hours. With increasing the aging time at the same temperature, the lamellar structure would occurred to the whole alloy, as illustrated in Fig. 3(b), which is a BF electron micrograph of a specimen aged at 400℃ for 24 hours. Figs. 3(c) and (d) are two SADPs taken from the precipitate marked as "B" in Fig. 3(b). From the camera length and the measurements of angles as well as d-spacings of the diffraction spots, the crystal structure of the precipitate was determined to be simple cubic with lattice parameter a=0.630nm, which corresponds to that of the A13 β-Mn[6-9]. Figs. 3(e) and (f) demonstrate

two SADPs taken from the precipitate marked as "R" in Fig. 3(b). Based on the analyses of the diffraction patterns, it is found that the precipitate is γ-brass having a $D8_3$ structure with lattice parameter a=0.872nm[3-4]. This indicates that the lamellar structure consists of β-Mn and γ-brass phases. Fig. 3(g), an SADP taken from an area covering two precipitates marked as "B" and "R" in Fig. 4(b), indicates that the orientation relationship between the β-Mn and γ-brass was $(001)_{\beta\text{-Mn}}//(0\,\bar{1}\,2)_{\gamma\text{-brass}}$, $(012)_{\beta\text{-Mn}}//(001)_{\gamma\text{-brass}}$, $(031)_{\beta\text{-Mn}}//(011)_{\gamma\text{-brass}}$ and $(010)_{\beta\text{-Mn}}//(021)_{\gamma\text{-brass}}$. It is worthwhile to note that the coexistence of the β-Mn and γ-brass has never been observed by other workers in the Cu-Al, Cu-Mn and Cu-Mn-Al alloy systems before.

When the alloy was aged at 650°C, the lamellar structure disappeared, and some coarse particles with a granular shape occurred within the $L2_1$ matrix, as shown in Fig. 4(a). Electron diffractions demonstrated that the coarse precipitates were β-Mn phase. Figs. 4(b) and (c) are two SADPs taken from the precipitate marked as "B" in Fig. 4(a) and its surrounding $L2_1$ matrix. It shows that the orientation relationship between the β-Mn and the $L2_1$ matrix is $[20\,\bar{1}]_{\beta\text{-Mn}}//[100]_{L2_1}$, $(102)_{\beta\text{-Mn}}//(002)_{L2_1}$ and $[100]_{\beta\text{-Mn}}//[201]_{L2_1}$, $(010)_{\beta\text{-Mn}}//(020)_{L2_1}$, which is similar to that found by the present workers in the Cu_2MnAl alloy[8]. Fig. 4(d) and (c) are the $(\bar{1}\,11)$ and (002) $L2_1$ DF electron micrograph, showing the presence of fine precipitates within the $L2_1$ domains. Fig. 4(e), a $(0\,\bar{2}\,0_1)$ L-J DF electron micrograph clearly reveals the presence of the fine L-J precipitates. In this figure, it is also seen that no evidence of the B2 phase could be detected.

Progressively higher temperature aging and quenching experiments indicated that the β-Mn precipitates were preserved up to 680°C. However, when the alloy was aged at 750°C for 30 minutes and then quenched, the microstructure was similar to that observed in the as-quenched alloy, as shown in Fig. 5.

五、Discussion

The as-quenched microstructure of the alloy was a mixture of (B2+$L2_1$+L-J) phases that is a remarkable feature in the present study. This result is quite different from that observed in the Cu_2MnAl alloy[1, 3-6], in which they observed that when the Cu_2MnAl alloy was solution heat-treated at a point in the β(disordered body-centered cubic) region and then quenched into iced brine rapidly, a $\beta \rightarrow B2 \rightarrow L2_1$ phase transition would occur during quenching. It means that the as-quenched microstructure of the Cu_2MnAl alloy was a single $L2_1$ phase. Furthermore, it is clearly seen in the $Cu_{3-x}Mn_xAl$ metastable phase diagram established by M. Bouchard and G. Thomas that the B2 phase could exist only at temperatures above 600°C[1]. Besides the more manganese content, the chemical composition of the present alloy is similar to that of the Cu_2MnAl alloy. It seems to imply that a higher manganese content in the Cu-Mn-Al alloy may favor the formation of extremely fine B2 precipitates within the $L2_1$ matrix during quenching. Here, it is interesting to discuss the characteristics of the formation of the B2 precipitates. The existence of the B2 precipitates in the as-quenched alloy may be attributed to two possible cases. (1) The B2 phase could exist only at higher temperature, which is similar to that in the Cu_2MnAl alloy. The higher manganese content in the present alloy resulted in an incompletely transformation from B2 to $L2_1$. Therefore, B2 phase was retained in the as-quenched alloy. (2) In contrast to the Cu_2MnAl alloy, the B2 phase indeed exists at lower temperature. Therefore, it is deduced that the B2 phase indeed exists at lower temperature, rather than retained during quenching.

A second important feature of the present study is that when the alloy was aged at temperature ranging from 400°C to 625°C, the lamellar structure of the (γ-brass ＋β-Mn) phases could be observed. This result is also different from that found by other workers in the aged Cu_2MnAl alloys [3-6]. In their studies, it is seen that the γ-brass precipitates were formed at 450°C or below; when the $Cu_{3-x}Mn_xAl$ alloy was aged from 460°C to 560°C, β-Mn precipitates started to occur and no evidence of the γ-brass precipitates could be detected. In order to clarify this difference, an STEM-EDS study was undertaken. The average concentrations of alloying elements obtained by analyzing a number of EDS spectra of each phase are listed in Table I. In Table I, it is clearly seen that the aluminum content in both of the γ-brass and the β-Mn is similar to that of the as-quenched alloy; while the manganese content of the γ-brass is much lower than that of the as-quenched

alloy. It is therefore suggested that along with the growth of the γ-brass precipitate, the surrounding region would be enriched in manganese. The enrichment of manganese would enhance the formation of manganese-enriched β-Mn precipitates at the regions contiguous to the γ-brass precipitates. Based on this proposition, it is expected that the coexistence of the (γ-brass +β-Mn) phases could also be observed by other workers in the $Cu_{3-x}Mn_xAl$ alloy. Therefore, it is reasonable to believe that a higher amount of manganese addition in the Cu-Mn-Al alloy should be favorable for the formation of the lamellar structure of the (γ-brass +β-Mn) phases.

TABLE I. Chemical Compositions of the Solution Heat-Treated Alloy, the γ-brass and the β-Mn Revealed by an EDS Spectrometer.

Heat Treatment	Phase	Chemical Compositions (at.%)		
		Cu	Mn	Al
solution heat-treated	$L2_1$+B2+L-J	48.52	27.78	23.72
400°C, 12h	γ-brass	72.20	4.34	23.46
400°C, 12h	β-Mn	5.55	71.10	23.35

六、Conclusion

On the basis of the above experimentally results, the phase transformations in the Cu-28Mn-24Al alloy could be summarized as follows:

1. The as-quenched microstructure of the alloy was a mixture of (B2+$L2_1$+L-J) phases, where the L-J phase and extremely fine B2 particles were formed within the larger $L2_1$ domains during quenching.
2. When the alloy was aged at 300°C or below, the fine B2 particles existing in the as-quenched alloy grew and the microstructure was still maintained the same as that in the as-quenched alloy.
3. At early stage of isothermal aging at 400°C, a mixture of (γ-brass +β-Mn) phases with a lamellar structure could be observed within the matrix. After prolonged the aging process at this temperature, the (γ-brass +β-Mn) lamellar structure had grown to a dimension of grains. Consequently, the stable microstructure of the alloy at 400°C was (γ-brass +β-Mn) phases.
4. Transmission electron microscopy observations indicated that the lamellar structure could exist up to 625°C. When the alloy was aged at 650°C, the β-Mn precipitates with a granular shape could be observed within the $L2_1$ matrix.
5. The microstructure of the alloy aged at 750°C and then quenched was ($L2_1$+B2) phases.
6. The phase transition sequence as the aging temperature was increased from 300 to 750°C was found to be (B2+$L2_1$+L-J) → ($L2_1$+γ-brass+β-Mn) → (γ-brass +β-Mn) → ($L2_1$+β-Mn) → (B2+$L2_1$+L-J).

七、Acknowledgements

The author is pleased to acknowledge the financial support of this research by the National Science Council, Republic of China under Grant NSC92-2216-E-009-026.

八、References

1. M.Bouchard and G.Thomas: *Acta Met*., 1975, vol. 23, pp. 1485-500.
2. Ye.G. Nesterenko, I.A. Osipenko and S.A. Firstov: *Fiz. Metal. Metalloved*., 1973, vol. 36, pp. 702-10.
3. R. Kozubski and J. Soltys: *J. Mater. Sci*., 1979, vol. 14, pp. 2296-302.
4. R. Kozubski and J. Soltys: *J. Mater. Sci*., 1982, vol. 17, pp. 1441-46.
5. R. Kozubski and J. Soltys: *J. Mater. Sci*., 1983, vol. 18, pp. 1689-97.
6. R. Kozubski, J. Soltys, J. Dutkiewicz and J. Morgiel: *J. Mater. Sci*., 1987, vol. 22, pp. 3843-46.
7. S. C. Jeng and T. F. Liu: *Metall. Trans. A*, 1995, vol. 26A, pp. 1353-65.
8. K.C. Chu and T.F. Liu, *Metall. Trans. A*,1999, vol 30A, pp. 1705-1716.
9. S.M.Allen and J.W.Cahn: Acta Metall., 24, 425. (1976)
10. Y.J.Chang: Acta Metall., 30, 1185. (1982)
11. C.C.Wu, J.S.Chou and T.F.Liu: Metall. Trans. A., 22A, 2265. (1991)
12. K. C. Chu, S. C. Jeng and T. F. Liu : Scripta Metall., 34, 83 (1996).

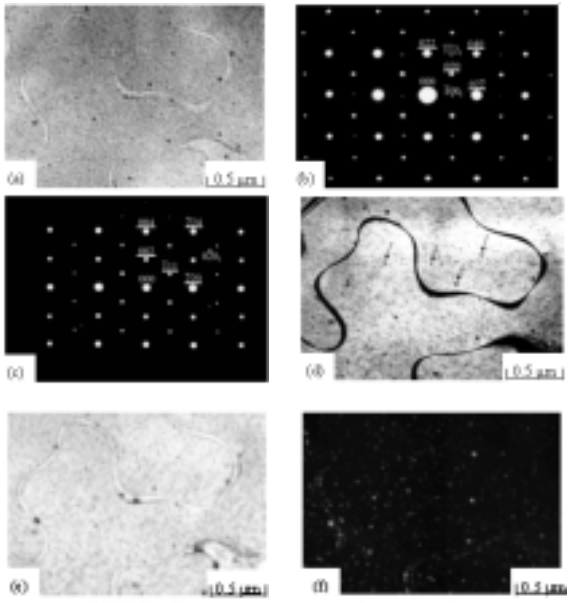

Fig. 1 Electron micrographs of the as-quenched alloy. (a) BF ; (b) and (c) two SADPs. The zone axes of the $L2_1$ phase are (b) [100] and (c) [110], respectively ($\underline{hkl}$= $L2_1$, hkl_1= L-J phase, 1:variant 1) ; (d) $(0\bar{2}0_1)$L-J DF ; (e) and (f) ($\bar{1}$ 11) and (002) $L2_1$ DF, respectively.

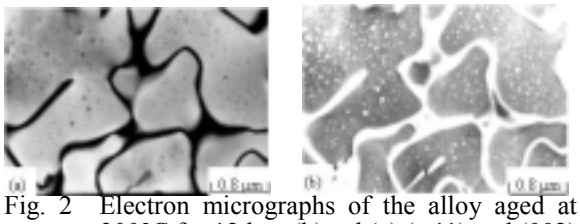

Fig. 2 Electron micrographs of the alloy aged at 300°C for 12 hrs. (b)and (c) ($\bar{1}$ 11) and (002) $L2_1$ DF, respectively.

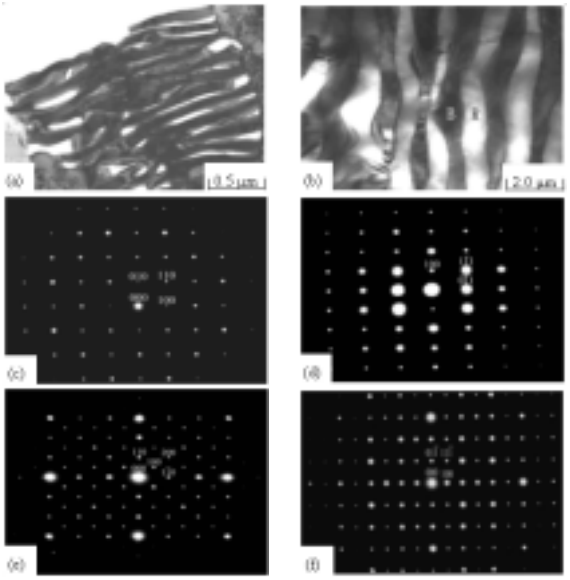

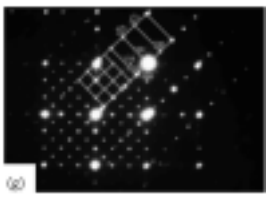

Fig. 3 Electron micrographs of the alloy aged at 400°C. (a) BF for 2 hrs ; (b) BF for 24 hrs ; (c) and (d) two SADPs taken from the area marked as "B" in (b). The zone axes are [001] and [011], respectively. (e) and (f) two SADPs taken from the area marked as "R" in (b). The zone axes are [001] and [011], respectively. (g) a SADP taken from the area covering "R" and "B" in (b). The zone axes for β -Mn and γ -brass are $[0\bar{1}2]$ and [001], respectively. ($\underline{hkl}$= β -Mn, hkl= γ -brass).

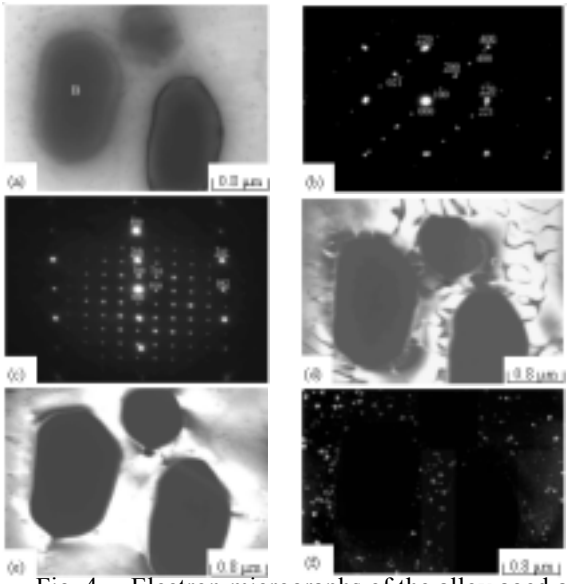

Fig. 4 Electron micrographs of the alloy aged at 650°C for 30 mins. (a) BF, (b) and (c) two SADPs taken from a precipitate marked as "B" and its surrounding $L2_1$ matrix. The zone axes are $[012]_{\beta\text{-Mn}}$, $[001]_{\beta\text{-Mn}}$ for β -Mn and $[001]_m$, $[0\bar{1}2]_m$ for matrix, respectively.($\underline{hkl}$: $L2_1$ matrix; hkl: β -Mn) (d) and (e) (111) and (002) $L2_1$ DF, respectively ; (f) (020_1)L-J DF.

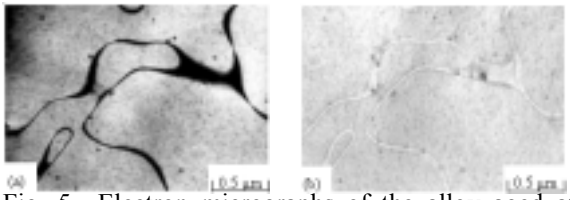

Fig. 5 Electron micrographs of the alloy aged at 750°C for 1hr. (a) and (b) ($\bar{1}$ 11) and (002) $L2_1$ DF, respectively